Hybrid Room: Does it Offer Better Accuracy in the Proximal Deployment of Infrarenal Aortic Endograft?

Louis Pruvot, Benjamin Lopez, Benjamin Oliver Patterson, Agathe de Préville, Richard Azzaoui, Thomas Mesnard, Jonathan Sobocinski

Hybrid room: Does it offer better accuracy in the proximal deployment of infrarenal aortic endograft?

L Pruvot[1], B Lopez[2], BO Patterson[3], A de Préville[1], R Azzaoui[1], T Mesnard[1,4], J Sobocinski[1,4]*

1. Service de chirurgie vasculaire, Centre de l'Aorte, CHU Lille, France
2. Laboratoire de Biologie Médicale, CH Dunkerque, Dunkerque, France.
3. Department of Vascular Surgery, University Hospital Southampton, United Kingdom
4. Univ. Lille, U1008 - Controlled Drug Delivery Systems and Biomaterials, F-59000 Lille, France

Louis Pruvot, MD, louis.pruvot@chru-lille.fr

Benjamin Lopez, MD, benjamin.lopez.86@gmail.com

Benjamin Oliver Patterson, PhD, benjamin.patterson@me.com

Agathe De Préville, MD, agathe.lechevalierdepreville@chru-lille.fr

Richard Azzaoui, MD, richard.azzaoui@chru-lille.fr

Thomas Mesnard, MD, thomas.mesn@gmail.com

Prof. Jonathan Sobocinski, MD, PhD, *Corresponding author

Mailing address: Service de chirurgie vasculaire, Centre de l'Aorte, CHU Lille, Université de Lille, France

mail-to: jonathan.sobocinski@univ-lille.fr

phone: +33 320 44 58 11

Total word count: 5337

Declaration of Conflict of interests: J Sobocinski is consultant for Cook Medical® and GE Healthcare®.

Abstract

Purpose This work aims to evaluate the impact of hybrid rooms and their advanced tools on the accuracy of proximal deployment of infrarenal bifurcated endograft (EVAR).

Methods A retrospective single centre analysis was conducted between January 2015 and March 2019 including consecutive patients that underwent EVAR. Groups were defined whether the procedure was performed in a hybrid operating room (HOR group) or using a mobile 2D fluoroscopic imaging system (non-HOR group). The accuracy of the proximal deployment was estimated by the distance (mm) between the bottom of the lowest renal artery (LwRA) origin and the endograft radiopaque markers parallax (LwRA/EDG distance) after curvilinear reconstruction. The impact of HOR on the LwRA/EDG distance was investigated using a multiple linear regression model. A composite "proximal neck"-related complications event was studied (Cox models).

Results Overall, 93 patients (87 %male, median age 73 years) were included with 49 in the HOR group and 44 in the non-HOR group. Preoperative CTA analysis of the proximal neck exhibited similar median length, but different median aortic diameter ($p=0.012$) and median beta angulation ($p=0.027$) between groups. The median LwRA/EDG distance was shorter in the HOR group (multivariate model, $p=0.022$). No difference in "proximal neck"-related complications was evidenced between the HOR and non-HOR groups (univariate analysis, $p=0.620$).

Median follow-up time was respectively 25 [14-28] and 36 months [23-44] in the HOR group and in the non-HOR group ($p<0.001$).

Conclusion HOR offer more accurate proximal deployment of infrarenal endografts, with however no difference in "proximal neck"-related complications between groups.

Key words: hybrid room, EVAR, proximal seal, image fusion, endograft deployment

Introduction

Endovascular aneurysm repair (EVAR) has become the most frequent treatment modality for infrarenal abdominal aortic aneurysm (AAA) (1). Nevertheless, it appears that the initial lower morbidity and mortality compared to open surgery is not sustained when considering long-term follow-up of randomised control trials (2,3). Long-term outcomes are closely related to the initial anatomical conditions and meeting the eligibility criteria of the devices, both merged into the instructions for use (IFU)'s book proposed by the manufacturers (4,5,6,7). Proximal type 1 endoleaks (type IA) after EVAR represent the main cause of late rupture (8,9,10,11).

Recent advances in Hybrid operating Rooms (H0R) include software that assists in endovascular navigation during the procedure. In addition to the well-known fusion software, that overlays the live fluoroscopy to the preoperative computed tomography angiogram (CTA) or the intraoperative cone beam computed tomography (CBCT), other tools such as orthogonal rings can also be manually or semi-automatically generated and added on the fusion mask to delineate anatomical zones of interest. The dissemination of use and access to H0R has already proven benefit for patients and medical staff in terms of radiation dose exposure, amount of iodine contrast injected and subsequent procedural duration (12,13,14,15); it also might reduce the number of additional endograft components implanted and enable immediate intraoperative correction when necessary (12).

In our centre, most EVAR procedures have been performed in a HOR (IGS 730 Discovery, GE Healthcare) since October 2012 incorporating a fusion mask and more recently integrated orthogonal rings.

This work aims to compare the accuracy of the proximal deployment of infrarenal bifurcated endograft completed with 2 different imaging systems, one with HOR including the dedicated above-mentioned software and one mobile imaging system with no advanced navigation software in a high-volume aortic centre.

Methods

Study group

Consecutive EVARs performed in a single tertiary referral centre from January 2015 to March 2019 was retrospectively included. Only patients with an available preoperative CTA (completed less than 6 months prior to the procedural time) and with slice thickness lower than 3mm were included. All patients had a CTA within the first 6 months postoperatively after EVAR.

Complex aortic aneurysms (thoraco-abdominal, para or juxta-renal aneurysms) treated with fenestrated and/or branched endograft, and aortic dissection were excluded from the study. All EVAR procedures were performed by the same surgical team. Groups were retrospectively defined according to the imaging system used for the procedure; for infra-renal aortic exclusion, the choice of the operating environment is randomly assigned depending on the HOR availability. The complex aortic exclusions are systematically performed in the HOR

This study was approved by the local Institutional Ethics Review Board.

Preoperative imaging

Pre and post-operative CTAs were analysed on a 3D workstation (iNuition Aquarius 3D Workstation TeraRecon Inc, San Mateo, Calif, USA) by the same operator trained in EVAR planning. Aortic and branch vessels centerline of flow (CLF) was automatically generated and modified if required. Anatomical characteristics of the infrarenal proximal neck were measured (outerwall proximal and distal diameters, length, alpha and beta angles, thrombus and calcifications percentage and thickness), as well as other anatomical variables (see appendix for method of measurements) were also recorded. All measurements were performed according to published reporting standards (16). In some situations the target sealing zone can be a straight aortic segment that is not just below the lowest renal artery but no patient had this aortic neck presentation and the intended sealing zone was located as close as possible to the lowest renal artery in all patients.

CTA image fusion and orthogonal rings– HOR procedures

Before the index EVAR the preoperative CTA was systematically loaded onto a dedicated workstation connecting to the imaging system of our HOR (Advantage Windows, GE Healthcare, Chalfont, UK) (EA-AW). The workstation includes dedicated software (*EVAR ASSIST*) that generates automatically a 3D volume rendering (VR) reconstruction with aortic and branch vessels CLF. Then, following those centrelines, circles named "orthogonal rings" can be drawn at the discretion of the operator to delineate anatomical regions of interest (arterial bifurcation, arterial lesion, sealing zones, etc.). These rings are in the orthogonal axis of the centrelines. Before the EVAR procedure, 2 orthogonal rings are drawn in order to be as precisely matched to the intended point of deployment of the leading edge of the endograft as possible: the first ring is drawn just below the bottom of the origin of the lowest renal artery (LwRA) and the second one delineates the LwRA ostium. Then, the best working projection is defined as the perpendicular plan of those 2 orthogonal rings (Figure 1) and the angulation of the simulated gantry is recorded for the procedure.

In addition, before completing the deployment of the proximal endograft, the position of the gantry can be adjusted and lined up to the orthogonal plan formed by the proximal markers of the endograft that is often slightly different after the stiff wires are introduced and a new angiogram can be performed to ensure accurate positioning (17).
Systematic meticulous analysis of the anatomy with delineation of the 'best working projection' is done preoperatively on a dedicated workstation; whatever the imaging system used afterwards

Surgical procedure

The hybrid endovascular suite in our institution (Discovery IGS 730, GE Healthcare, Chalfont St Giles, UK) is equipped with a 30x30 centimetres flat panel detector and an EA-AW console with the Innova Vision 2® software allowing CTA image fusion process. In this HOR, all EVAR are controlled intraoperatively with a CBCT and a completion angiogram or with a contrast-enhanced-CBCT. The standard fluoroscopic 2D imaging system is a mobile X-ray image intensifier (OEC 9900 Elite GE Healthcare) with a floating table (STILLE, Se). All the bifurcated endografts implanted during the period of the study were Zenith Low Profile® (LP), Zenith Alpha® or Zenith Flex®(Cook INC, Bloomington, IN, USA).

Data collection

Population characteristics, intraoperative data, perioperative management and follow-up included rates of early (<30-day) and late (> 30-day) adverse events and secondary interventions were reported. Intraoperative data included: endografts characteristics, intraoperative preplanned and unplanned additional procedures, operating time, iodinated contrast volume injected, radiation dose (Gy.cm2), fluoroscopy time and intraoperative adverse events (defined as type I/III endoleaks, endograft kink or occlusion, target vessels coverage, access vessels complications).

Postoperative imaging

All patients had a postoperative CTA (slice thickness lower than 3 mm). The postoperative CTA was performed within the first month following EVAR in the non-HOR group, or sooner if a complication was suspected (in both groups). A contrast-enhanced ultrasound (CEUS) was completed prior to discharge for all patients, then at 6 months and yearly thereafter.

Thirty-day postoperative CTA for patients in the HOR group was delayed to 6 months if no complication were suspected on the intraoperative CBCT nor on CEUS. In the non-HOR group, all patients had a postoperative CTA in the month following surgery.

All the postoperative CTA were analysis on a 3D workstation (Terarecon) by an experienced operator in EVAR planning. The distance between the lower edge of the LwRA and the proximal gold markers of the endograft was measured after CLF reconstruction. An optimal positioning is defined as a LwRA/EDG distance ≤2mm. Other relevant data as the maximal aortic diameter, stent kinks or/and evidence of type IA endoleak were collected.

Primary and secondary endpoints

The accuracy of the proximal bifurcated endograft position was estimated by the distance between the lower edge of the LwRA and the parallax of the proximal gold markers of the endograft (LwRA/EDG distance) and was analysed between groups in a multivariate model to depict any predictors.

Any element during follow-up related to the proximal aortic neck including early or late proximal type 1 endoleak detection or additional procedure such as additional ballooning, stenting or fenestrated cuff extension at this level have been combined in a composite endpoint named "proximal neck" -related complications.

Statistical analysis

Continuous variables are quoted as the median (interquartile range (IQR)) and categorical variables are presented as absolute numbers (percentage).
Comparison of demographic, pre-operative morphological and intra-operative data were performed using Student's T for continuous covariates and the Chi-square or Fisher's exact tests for categorical covariates.

First, the dependent variable "LwRA/EDG distance" was investigated through linear regression models. The multivariate analysis included all variables considered significant in univariate analyses ($p<0.20$).
Factors associated with the dependent variable "LwRA/EDG distance" were investigated through multiple linear regression (PROC MIXED in SAS®) and results are expressed as the increase in LwRA/EDG distance per unit change in the explanatory variable. Univariate analyses were first conducted with graphical assessment of the regression assumptions. Multivariate models were then built by first including all variables considered with a p-value <0.20 in univariate analyses ($p<0.20$) and then using a backward selection to reduce the model ($p<0.05$ threshold).
Because of a direct relationship between the variable "time interval between EVAR and postoperative CTA" and the LwRA/EDG distance, this variable was systematically forced into

the multivariate model. In order to meet linearity requirements, the time was modeled as a piecewise linear effect (2 linear segments with a 12-months cut-off).

The presence of interactions between the delay and all other variables was systematically investigated.

The absence of collinearity was systematically verified by calculating the Variance Inflation Factor.

Secondarily, survival analyses were conducted for the occurrence of “proximal neck” - related complications (PROC PHREG in SAS®). In respect to the limited number of events, only the HOR/non-HOR use and the LwRA/EDG distance covariates were tested in univariate analyses. Event-free survival curves were estimated by the Kaplan-Meier method and compared with the log-rank test. Median follow-up time was estimated with the reverse Kaplan-Meier method. Univariate Cox analyses were also performed. The log-linearity assumption for continuous variables and the proportional hazard assumption were tested by Kolmogorov-type supremum tests.

A p-value of <0.05 was considered as statistically significant for all analyses.

Results

Ninety-three patients were included, 49 in the HOR group and 44 in the non-HOR group, while 826 endovascular aortic cases were performed in our center over the same period of time. Demographics and anatomical characteristics are listed in Table 1. The proximal neck median diameter was significantly greater in the non-HOR group (24.0mm (22.0-25.0) vs 22.0mm (21.0-24.0); p=0.012), whereas the median beta angle was superior in the HOR group (31.5° (15.5, 43.0) vs 22.0° (13.0, 30.0); p=0.027). The two groups were comparable with respect to the other anatomical variables recorded. In one patient (non-HOR group) with a history of chronic renal failure requiring dialysis, the renal arteries were covered to get a proper proximal seal below the superior mesenteric artery (SMA).

Procedural data are presented in Table 2. Median surgical time (HOR group: 82.0 min (65.0, 110.0) vs non-HOR group: 90.0 min (80.0, 120.0); $p>0.05$) and median radiation dose (HOR group: 21.8 Gy.cm2 (12.3, 49.4) vs non-HOR group: 29.0 Gy.cm2 (17.3, 71.8); $p>0.05$) were similar in each group, whereas median fluoroscopic time was significantly higher in the HOR group (15.4 min (11.5, 25.0) vs 10.5 min (4.9, 15.4); $p=0.014$). In the HOR group, 41 Zenith alpha® and 8 Zenith Flex® were implanted and in the non-HOR group 24 Zenith alpha®, 13 Zenith Flex® and 7 Zenith LP® were implanted.

Most of pre-planned additional procedures were unilateral or bilateral iliac branch devices (n=10, all for patients in the HOR group), and endograft bifurcation kissing stenting (2 in the HOR group and 4 in the non-HOR group). A patient with a low accessory renal artery origin from the infrarenal aorta had a single chimney graft (HOR group). Intraoperative adverse events were not different between the two groups (HOR group: n=3 (6.1%) vs non-HOR: group n=4 (9.5%); $p=1.000$). A type IA endoleak was depicted on the intraoperative CBCT in 1 patient in the HOR group and immediately corrected with a Palmaz stent (Cordis, Fremont, Calif) and 2 in the non-HOR group treated with adjunctive compliant balloon expansion (Coda Balloon, Cook Medical, Bloomington, Indiana, USA). After initial correction, no persistent type IA endoleak was depicted on the final completion angiogram.

The other intraoperative adverse events were access vessels issues due to percutaneous closure system failure requiring open surgical repair (1 patient of the HOR group and 1 of the non-HOR group), and a case of incorrect contralateral limb deployment requiring iliac limb explantation through a left Rutherford-Morrison incision (non-HOR group).

Postoperative data are presented in Table 3. Postoperative adverse events rates (including early and late adverse events) were similar in each group (HOR group: n=5 (10.2 %) vs non-HOR group: n=5 (11.4 %); p>0.05). Early adverse events occurred in three patients including one acute postoperative lower limb ischemia (HOR group), one acute renal failure that didn't required dialysis (non-HOR group) and one groin hematoma (non-HOR group).

Most of the late adverse events were device thrombosis (n=6 (6.5%)), including 1 internal iliac branch (HOR group), 3 iliac limbs (1 in HOR group and 2 in non-HOR group), 1 main endograft body (HOR group) and 1 renal chimney graft (HOR group). Other late adverse events were not device-related with 1 atherosclerotic acute lower limb ischemia (non-HOR group). A type IA endoleak was depicted in 1 (2.1%) patient of the HOR group and 2 (5.3%) patients of the non-HOR group during follow-up.

The median LwRA/EDG distance was 1.0 mm (0.5, 2.0) and 2.0mm (1.5, 3.5) respectively in the HOR group and the non-HOR group (p<0.001). Sixty-six patients (71.0%) had an optimal endograft positioning (meaning the distance LwRA/EDG ≤2mm) (HOR group: n=40 (81.6%), non-HOR group: n=26 (59.1%)) on the first postoperative CTA.

Neck characteristics and postoperative LwRA/EDG distance of patients presenting a type IA (intraoperative or during follow-up) are available in supplementary Table 1.

The rate of early and late secondary interventions (detailed in Table 4) was not different between groups (HOR group: n=9 (18.4%) vs non-HOR group: n=5 (11.4%); p>0.05). Median follow-up was 25 months (14, 28) in the HOR group and 36 months (23, 44) in the non-HOR group (p<0.001).

In a multivariate analysis (Supplementary Table 2), it appeared that performing EVAR cases in HOR was significantly correlated to a reduction in the LwRA/endograft distance with an increasing factor (IF) of -0,69 mm (95% CI (-1.28-0.10); p=0.022), likewise a CTA performed after 12 months from EVAR was associated with an increasing LwRA/endograft distance (IF= +0.12 mm, 95% CI (0.05-0.18); p<0.001).

Using the Kaplan-Meier estimator the rate of freedom from “proximal-neck” -related complications was 95.8% (IC95% [84.4; 98.9]) at 12 and was stable at two years due to the few number of events (p=0.615 for the comparison of survival curves) (Figure 2).

In univariate Cox models, no significant difference was found between the HOR and non-HOR groups (HR=0.636, 95%CI [0.106-3.811]; p=0.620). An initial optimal EDG positioning (LwRA/EDG distance ≤ 2mm) was not significantly associated with a lower rate of “proximal neck”-related complications (HR=0.450, CI95% [0.052; 3.866], p=0.467).

Discussion

This study compares the accuracy of proximal bifurcated endograft positioning when EVAR procedures are performed in HOR (associated with the use of image fusion and orthogonal rings (HOR group)) or in operating rooms using a standard fluoroscopic 2D imaging system (non-HOR group), in a high-volume aortic centre. This was estimated using the LwRA/EDG distance measured on the postoperative CTA and was analyzed in a multivariate model.

The LwRA/EDG distance was lower in the HOR group compared to the other group after adjusted multivariate analysis (IF= -0.69 mm, 95% CI (-1.28-0.10); p=0.022), but no significant difference was found in the occurrence of early and late type IA endoleak between groups (HR=0.636, 95%CI (0.106-3.811); p=0.620).

More than 2500 EVAR cases have been performed so far in our centre since the beginning of our experience in 1995. The low number of patients included over the period of the study as regard of the total number of patients treated with EVAR was mostly explained by the ability to have access to the early postoperative CTA.

Since 2012, a hybrid operating room dedicated to vascular interventions has been available in our institution and has become the preferred environment to perform endovascular aortic repairs. Prior to 2012, all cases from whether straightforward or complex were managed with a standard fluoroscopic 2D imaging system; since then, few standard cases are still performed with this modality when the HOR is not available (149 EVAR cases since 2012 with a decreasing trend over years).

The maturation of the learning curve of our surgical team promotes systematic and meticulous evaluation of the aortic anatomy whichever environment is used to achieve the procedure.

The application of anatomical guidelines to select and treat patients with aortic endograft influences the efficacy and durability of EVAR (4). Meticulous preoperative anatomical aortic studies achieved with 3D imaging workstations is therefore mandatory to depict adequate anatomy prior EVAR (18,19).

Despite performing this essential step, an endograft deployed a few millimetres below the expected target position can result in a reduced and therefore insufficient proximal seal length, less than the 15mm recommended by most of the manufacturers. This might subsequently affect long-term durability. A perfect initial positioning is therefore crucial, and deployment of the endograft as close as possible to the LwRA, even if the proximal sealing zone length is greater than 15 mm, will optimise the wall apposition of the endograft.

With this in mind, the proximal and distal best working positions angulations, determined on the preoperative CTA, are manually reported for the operator's use on a worksheet accessible during the procedure in order to avoid parallax error in endograft deployment.

The relationship between the endograft apposition, position, and expansion in the aortic neck and post-EVAR complications defined as type IA endoleak and/or caudal endograft migration has previously been studied (20). Post-EVAR complications were significantly associated with a change in position of the endograft fabric relative to the renal arteries over time. We demonstrated that a CTA performed 12 months after EVAR was associated with an increasing LwRA/EDG distance (increasing factor IF=0.12, 95% CI (0.05-0.18); $p<0.001$) which may reflect a slight but significant endograft migration over time.

Thus, an initial accurate endograft position is important to reduce the risk of proximal leak during follow-up.

In their series, Schuurmann et al (20) included 81 patients, treated with various brands of endografts, where the LwRA/endograft distance just after the procedure was between 0 and 3 mm in 44%, too high (partially covering renal artery) in 30% and too low position (distance >3mm) in 26% of patients. Bastos Gonçalves *et al.* (21) reported similar results with 29% patients (of 131 patients included) observed as having a postoperative LwRA/endograft distance of >5mm in patient treated with the Excluder endograft (W.L. Gore & Assoc, Flagstaff, Ariz). These latter series did not specify whether the EVAR procedure was performed in a HOR or not.

In the present study, the optimal endograft positioning was achieved in 94% (n=46/49) in the HOR group and 75% (n=33/44) in the non-HOR group, when considering a target optimal gap ≤3mm below the lowest renal artery and the endograft. In the Bastos Gonçalves et al. study, EVAR procedures were probably not performed in HOR as the period of inclusion was before HOR generalization (from 2004 to 2011), and their results are close to our findings in the non-HOR group.

All the bifurcated endografts implanted in the present report were Cook® devices which IFU's state that the proximal gold markers are located within 2mm of the most proximal aspect of the fabric. In reality these markers are probably less than 0.5mm from the most proximal edge of the fabric (Figure 3), that's why in order to optimize the proximal sealing we systematically intend to deploy the parallax of the markers of the proximal stent as close as possible to the lower edge of the LwRA without considering that manufacturer's instruction as relevant.

Despite a benefit in terms of endograft positioning the present comparative study has not highlighted any clinical benefit of performing EVAR in an HOR on the postoperative risk of type IA endoleak.

Intraoperative type IA endoleak was depicted in 3 cases (3.2%), adjunctive manoeuvres were necessary to correct all of them with no persistent endoleak on final completion angiogram. In the literature, the incidence of intraoperative type IA endoleak is probably underestimated depending on whether cases are recorded before or after treatment attempt (type IA endoleak are defined as persistent in this setting). Thus, the intraoperative type IA endoleak rate varies from 3.3% to 22.6% in reports dealing specifically with intraoperative type IA endoleaks (22,23,24).

The difference in LwRA/endograft distance observed between groups was not related to inter-operator variability since the procedures were performed by the same surgical team, strictly following the manufacturer's IFU in both groups. Schuurmann et al. (25) previously described a semiautomated method for measuring the postoperative distance between the LwRA and the endogaft fabric and showed that low endograft deployment was more frequently associated with increased infrarenal angulation. In our series, the proximal endograft positioning was superior in the HOR group despite a beta angle that was significantly steeper reflecting more challenging aortic anatomies in this latter group.

Moreover, the median proximal sealing zone length was greater in the HOR group, although not statistically significant, but the LwRA/endograft distance was significantly shorter in this group. In our series, a good median proximal sealing zone length was achieved in both groups (HR group: 36.0 (23.0, 43.0) vs non-HR group: 30.0 (25.0, 43.0)). This reflects the practice of our institution to perform EVAR only in case of favorable anatomies. We believe that no compromise should be made in case of calcification/thrombus and/or irregular diameters within aortic necks shorter than 15 mm. Otherwise these cases are managed with fenestrated endografts or open repair.

As far as we know the comparison of the proximal positioning of an infrarenal bifurcated endograft between HOR and standard fluoroscopic 2D imaging system has not been reported yet.

Several advantages of HOR for EVAR procedures have already been demonstrated in terms of radiation dose exposure, iodine contrast volume injected (13,15,26) and also in complex cases to ease the endovascular navigation and the target vessels catheterization (27). For all these elements, HOR represent a valuable environment to perform aortic endovascular procedures.

Nevertheless, current imaging fusion software tool presents potential important flaws as the software does not manage yet vessel displacement/distortions due to the rigidity of the endovascular material inserted within the vessel (17,28,29*).* To correct this mismatch, a DSA acquisition is usually performed after the insertion of the delivery system based on the calculated best working position (usually with a cranial incidence) to confirm the renal artery position, and then the mask and the orthogonal rings are then adjusted if necessary. After the opening of the proximal bare stent and the first covered stent, the cranial incidence is adjusted if necessary, to align the paralax of the gold markers. There is often a discrepancy between the plan of the gold markers and the orthogonal rings placed below the LwRA. This might be due as exposed above to the distortion of the anatomy and also might be influenced by the orientation of the delivery system that is not always parallel to the aortic centreline.

Despite these needed adjustments of the fusion mask and orthogonal rings, the use of 3D guidance in HOR become the standard of care in our daily practice for EVAR procedures.

In the present report, it is of note the fluoroscopy time, radiation exposure and iodinated contrast volume injection were not different between groups, but more patients in the HOR received more frequently unilateral or bilateral iliac branch devices concomitantly to EVAR in the HOR group.

Moreover, systematic CBCT were completed at the end of the procedure to assess the endovascular reconstruction adding a significant amount of radiation dose and contrast volume.

This study potentially shows limitations as it presents results from a retrospective and monocentric experience. Groups of patients were not completely comparable toward preoperative aortic anatomies, since more potential complicated EVAR cases were performed in the HOR.

Another potential bias was the difference between groups toward the time interval between EVAR and postoperative CTA, an independent factor that would affect (increase) the LwRA/EDG distance, although this element was considered and thus adjusted in the multivariate analysis.

At last, the influence of the type of delivery system of the endograft have been taken into consideration although it may affect the precision of endograft placement. Anyway, we believe that operator’s volume with a type of endograft is a major point in endograft deployment accuracy.

Conclusion

The use of image fusion-based roadmapping and orthogonal rings as markers in a hybrid operating room environment during EVAR procedures promotes accurate proximal aortic bifurcated endograft positioning. Characterising the subsequent clinical benefit of this would require further investigations in larger cohorts.

References

1. Dua A, Kuy S, Lee CJ, Upchurch GR, Desai SS. Epidemiology of aortic aneurysm repair in the United States from 2000 to 2010. J Vasc Surg. 2014;59:1512-7.

2. EVAR trial participants. Endovascular aneurysm repair versus open repair in patients with abdominal aortic aneurysm (EVAR trial 1): randomised controlled trial. Lancet Lond Engl. 2005;365:2179-86.

3. Brown LC, Powell JT, Thompson SG, Epstein DM, Sculpher MJ, Greenhalgh RM. The UK EndoVascular Aneurysm Repair (EVAR) trials: randomised trials of EVAR versus standard therapy. Health Technol Assess Winch Engl. 2012;16:1-218.

4. Schanzer A, Greenberg RK, Hevelone N, Robinson WP, Eslami MH, Goldberg RJ, et al. Predictors of abdominal aortic aneurysm sac enlargement after endovascular repair. Circulation. 2011;123:2848-55.

5. De Martino RR, Brooke BS, Robinson W, Schanzer A, Indes JE, Wallaert JB, et al. Designation as « unfit for open repair » is associated with poor outcomes after endovascular aortic aneurysm repair. Circ Cardiovasc Qual Outcomes. 2013;6:575-81.

6. Chaikof EL, Fillinger MF, Matsumura JS, Rutherford RB, White GH, Blankensteijn JD, et al. Identifying and grading factors that modify the outcome of endovascular aortic aneurysm repair. J Vasc Surg. 2002;35:1061-6.

7. Moll FL, Powell JT, Fraedrich G, Verzini F, Haulon S, Waltham M, et al. Management of abdominal aortic aneurysms clinical practice guidelines of the European society for vascular surgery. Eur J Vasc Endovasc Surg Off J Eur Soc Vasc Surg. 2011;41:S1-58.

8. Powell JT, Sweeting MJ, Ulug P, Blankensteijn JD, Lederle FA, Becquemin J-P, et al. Meta-analysis of individual-patient data from EVAR-1, DREAM, OVER and ACE trials

comparing outcomes of endovascular or open repair for abdominal aortic aneurysm over 5 years. Br J Surg. 2017;104:166-78.

9. Antoniou GA, Georgiadis GS, Antoniou SA, Kuhan G, Murray D. A meta-analysis of outcomes of endovascular abdominal aortic aneurysm repair in patients with hostile and friendly neck anatomy. J Vasc Surg. 2013;57:527-38.

10. Bastos Goncalves F, Hoeks SE, Teijink JA, Moll FL, Castro JA, Stolker RJ, et al. Risk factors for proximal neck complications after endovascular aneurysm repair using the endurant stentgraft. Eur J Vasc Endovasc Surg Off J Eur Soc Vasc Surg. 2015;49:156-62.

11. Zacharias N, Warner CJ, Taggert JB, Roddy SP, Kreienberg PB, Ozsvath KJ, et al. Anatomic characteristics of abdominal aortic aneurysms presenting with delayed rupture after endovascular aneurysm repair. J Vasc Surg. 2016;64:1629-32.

12. Varu VN, Greenberg JI, Lee JT. Improved efficiency and safety for EVAR with utilization of a hybrid room. Eur J Vasc Endovasc Surg Off J Eur Soc Vasc Surg. 2013;46:675-9.

13. Hertault A, Maurel B, Sobocinski J, Martin Gonzalez T, Le Roux M, Azzaoui R, et al. Impact of hybrid rooms with image fusion on radiation exposure during endovascular aortic repair. Eur J Vasc Endovasc Surg Off J Eur Soc Vasc Surg. 2014;48:382-90.

14. Dias NV, Billberg H, Sonesson B, Törnqvist P, Resch T, Kristmundsson T. The effects of combining fusion imaging, low-frequency pulsed fluoroscopy, and low-concentration contrast agent during endovascular aneurysm repair. J Vasc Surg. 2016;63:1147-55.

15. Maurel B, Martin-Gonzalez T, Chong D, Irwin A, Guimbretière G, Davis M, et al. A prospective observational trial of fusion imaging in infrarenal aneurysms. J Vasc Surg. 2018;68:1706-1713.

16. Chaikof EL, Blankensteijn JD, Harris PL, White GH, Zarins CK, Bernhard VM, et al. Reporting standards for endovascular aortic aneurysm repair. J Vasc Surg. 2002;35:1048-60.

17. Maurel B, Hertault A, Gonzalez TM, Sobocinski J, Le Roux M, Delaplace J, et al. Evaluation of visceral artery displacement by endograft delivery system insertion. J Endovasc Ther Off J Int Soc Endovasc Spec. 2014;21:339-47.

18. Sobocinski J, Chenorhokian H, Maurel B, Midulla M, Hertault A, Le Roux M, et al. The benefits of EVAR planning using a 3D workstation. Eur J Vasc Endovasc Surg Off J Eur Soc Vasc Surg. 2013;46:418-23.

19. Parker MV, O'Donnell SD, Chang AS, Johnson CA, Gillespie DL, Goff JM, et al. What imaging studies are necessary for abdominal aortic endograft sizing? A prospective blinded study using conventional computed tomography, aortography, and three-dimensional computed tomography. J Vasc Surg. 2005;41:199-205.

20. Schuurmann RCL, van Noort K, Overeem SP, van Veen R, Ouriel K, Jordan WD, et al. Determination of Endograft Apposition, Position, and Expansion in the Aortic Neck Predicts Type Ia Endoleak and Migration After Endovascular Aneurysm Repair. J Endovasc Ther Off J Int Soc Endovasc Spec. 2018;25:366-75.

21. Bastos Gonçalves F, van de Luijtgaarden KM, Hoeks SE, Hendriks JM, ten Raa S, Rouwet EV, et al. Adequate seal and no endoleak on the first postoperative computed tomography angiography as criteria for no additional imaging up to 5 years after endovascular aneurysm repair. J Vasc Surg. 2013;57:1503-11.

22. Tan T-W, Eslami M, Rybin D, Doros G, Zhang WW, Farber A. Outcomes of patients with type I endoleak at completion of endovascular abdominal aneurysm repair. J Vasc Surg. 2016;63:1420-7.

23. Millen AM, Osman K, Antoniou GA, McWilliams RG, Brennan JA, Fisher RK. Outcomes of persistent intraoperative type Ia endoleak after standard endovascular aneurysm repair. J Vasc Surg. 2015;61:1185-91.

24. Sampaio SM, Shin SH, Panneton JM, Andrews JC, Bower TC, Cherry KJ, et al. Intraoperative endoleak during EVAR: frequency, nature, and significance. Vasc Endovascular Surg. 2009;43:352-9.

25. Schuurmann RCL, Overeem SP, Ouriel K, Slump CH, Jordan WD, Muhs BE, et al. A Semiautomated Method for Measuring the 3-Dimensional Fabric to Renal Artery Distances to Determine Endograft Position After Endovascular Aneurysm Repair. J Endovasc Ther Off J Int Soc Endovasc Spec. 2017;24:698-706.

26. Tacher V, Lin M, Desgranges P, Deux J-F, Grünhagen T, Becquemin J-P, et al. Image guidance for endovascular repair of complex aortic aneurysms: comparison of two-dimensional and three-dimensional angiography and image fusion. J Vasc Interv Radiol JVIR. 2013;24:1698-706.

27. Hertault A, Sobocinski J, Spear R, Azzaoui R, Delloye M, Fabre D, et al. What should we expect from the hybrid room? J Cardiovasc Surg (Torino). 2017;58:264-9.

28. Schulz CJ, Schmitt M, Böckler D, Geisbüsch P. Fusion Imaging to Support Endovascular Aneurysm Repair Using 3D-3D Registration. J Endovasc Ther Off J Int Soc Endovasc Spec. 2016;23:791-9.

29. Kauffmann C, Douane F, Therasse E, Lessard S, Elkouri S, Gilbert P, et al. Source of errors and accuracy of a two-dimensional/three-dimensional fusion road map for endovascular aneurysm repair of abdominal aortic aneurysm. J Vasc Interv Radiol JVIR. 2015;26:544-51.

Table/Figure legends

Table 1 Demographics and preoperative morphological data of 93 patients undergoing EVAR stratified by the type of imaging system used during procedure

Table 2 Procedural data of 93 patients undergoing EVAR stratified by the type of imaging system used during procedure

Table 3 Postoperative data of 93 patients undergoing EVAR stratified by the type of imaging system used during procedure

Table 4 Details of secondary interventions of 93 patients undergoing EVAR stratified by the type of imaging system used during procedure

Figure 1

The best working position for proximal endograft deployment defined as perpendicular plan of the orthogonal rings placed at the level of the aorta just below the lowest renal artery and at the ostium of the lowest renal artery

Figure 2

Cumulative Kaplan-Meier survival estimates of freedom from "proximal neck"-related complications (including early and late type IA endoleaks) of 93 patients treated in a hybrid room (HOR group) or with a mobile 2D fluoroscopic imaging system (non-HOR group)

Supplementary Table 1 Preoperative and postoperative anatomical characteristics of patients presenting an intraoperative or postoperative type IA endoleak

Supplementary Table 2: Multivariable associations with an increasing LwRA/EDG distance

Figure 3

Location of the proximal gold markers (red arrows) of Cook® Medical bifurcated endografts from the most proximal aspect of the fabric

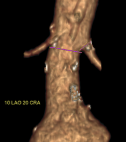
10 LAO 20 CRA

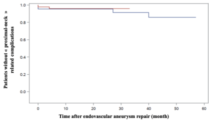

No. at risk

HOR group	44	39	29	21	17	7	0
Non-HOR group	48	37	27	9	0		

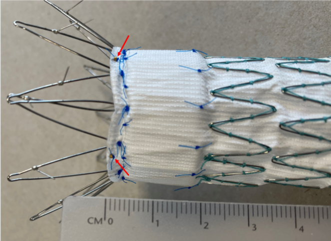
CM 0 1 2 3 4

Table 1 Demographics and preoperative morphological data of 93 patients undergoing EVAR stratified by the type of imaging system used during procedure

	HOR (n=49)	Non-HOR (n=44)	Total (n=93)
Sex (female)	5 (10.2 %)	1 (2.3 %)	0.201
Age (years)	75.0 (69.0, 81.0)	71.0 (65.0, 78.0)	0.070
Previous aortic disease	1 (2.0 %)	1 (2.3 %)	1.000
Aneurysm location			0.208
Infrarenal aorta	44 (89.8 %)	43 (97.7 %)	
Common iliac artery	5 (10.2 %)	1 (2.3 %)	
Maximal aneurysm diameter (mm)	55.0 (50.0, 62.0)	54.0 (50.5, 59.0)	0.580
Infrarenal aortic neck length (mm)	36.0 (23.0, 43.0)	30.0 (25.0, 43.0)	0.855
Target vessel for proximal positioning			0.669
Lower edge of the RRA	20 (40.8 %)	16 (36.4 %)	
Lower edge of the LRA	29 (59.2 %)	27 (61.4 %)	
Lower edge of the SMA	0 (0.0 %)	1 (2.3 %)	
Proximal edge diameter of the aortic neck (mm)	22.0 (21.0, 24.0)	24.0 (22.0, 25.0)	0.012
Distal edge diameter of the aortic neck (mm)	23.0 (21.0, 25.0)	24.0 (22.0, 25.0)	0.071
Neck features			0.065
Tubular	41 (83.7 %)	33 (76.7 %)	
Angled	3 (6.1 %)	0 (0.0 %)	
Conical	5 (10.2 %)	7 (16.3 %)	
Funnel,shaped	0 (0.0 %)	3 (7.0 %)	
Alpha angle (°)	11.0 (3.0, 20.0)	13 (8.0, 22.5)	0.875
Beta angle (°)	31.5 (15.5, 43.0)	22.0 (13.0, 30.0)	0.027
Circumferential calcification percentage (aortic neck)			0.131
<25%	35 (71.4 %)	25 (56.8 %)	
25.50%	12 (24.5 %)	12 (27.3 %)	
>50%	2 (4.1 %)	7 (15.9 %)	
Circumferential thrombus percentage (aortic neck)			0.376
<25%	38 (80.9 %)	34 (82.9 %)	
25.50%	8 (17.0 %)	4 (9.8 %)	
>50%	1 (2.1 %)	3 (7.3 %)	

HOR: Hybrid operating room, LRA: left renal artery, non-HOR: mobile 2D fluoroscopic imaging system RRA: right renal artery, SMA: superior mesenteric artery patient with chronic renal failure requiring dialysis, renal arteries were covered

Continuous data are presented as the median (Inter Quartile Range) and categorical data as counts (percentage)

Table 2 Procedural data of 93 patients undergoing EVAR stratified by the type of imaging system used during procedure

	HOR (n=49)	Non-HOR (n=44)	*p*
Emergent cases*	3 (6.1 %)	1 (2.3 %)	0.619
Access vessels			<0.001
Percutaneous approach	38 (77.6 %)	7 (15.9 %)	
Surgical cutdown	9 (18.4 %)	37 (84.1 %)	
Both	2 (4.1 %)	0	
Operating time (min)	82.0 (65.0, 110.0)	90.0 (80.0, 120.0)	0.879
Fluoroscopy time (min)	15.4 (11.5, 25.0)	10.5 (4.9, 15.4)	0.014
Radiation dose (Gy.cm^2)	21.8 (12.3, 49.4)	29.0 (17.3, 71.8)	0.325
Iodinated contrast volume (mL)	70.0 (57.0, 80.0)	80.0 (60.0, 100.0)	0.343
Intraoperative endovascular additional procedures	16 (38.3%)	9 (22.0%)	0.097
Preplanned			
Unilateral iliac branch device	8 (16.3%)	0	
Bilateral iliac branch devices	2 (4.1%)	0	
Endograft bifurcation kissing stenting	2 (4.1%)	4 (9.1%)	
External iliac artery stenting	1 (2.0%)	2 (4.5%)	
Internal iliac artery embolisation	0	1 (2.3%)	
Renal chimney	1 (2.0%)	0	
Unplanned			
Iliac limb endograft extension	1 (2.0%)	0	
Proximal seal palmaz stenting	1 (2.0%)	0	
Proximal seal compliant balloon expansion	0	2 (4.5%)	
Intraoperative adverse events	3 (6.1%)	4 (9.1%)	1.000
Type IA endoleak	1 (2.0%)	2 (4.5%)	
Type IB endoleak	1 (2.0%)	0	
Access vessels issues	1 (2.0%)	1 (2.3%)	
Iliac limb extraction	0	1 (2.3%)	

HOR: Hybrid operating room, non-HOR: mobile 2D fluoroscopic imaging system

Continuous data are presented as the median (Inter Quartile Range) and categorical data as counts (percentage)

* symptomatic or ruptured aneurysm

Table 3 Postoperative data of 93 patients undergoing EVAR stratified by the type of imaging system used during procedure

	HOR (n=49)	Non-HOR (n=44)	*p*
Early and late adverse events	5 (10.2 %)	5 (11.4 %)	1.000
Postoperative CTA analysis			
Time from procedure to postoperative CTA (months)	5.0 (0.0, 9)	1.0 (0.0, 9.5)	0.442
Slice thickness ≤1mm	38 (77.6 %)	32 (74.4 %)	0.725
CTA with arterial phase	41 (83.7 %)	35 (81.4 %)	0.774
Difference in diameter compared to preoperative CTA (mm)	0 (. 1, 2)	0 (-1, 2)	0.951
Type IA endoleak	1 (2.1 %)	2 (5.3 %)	0.581
Kink	2 (4.1 %)	1 (2.3 %)	1.000
LwRA/EDG distance* (mm)	1.0 (0.5, 2.0)	2.0 (1.5, 3.5)	0.001
Early and late secondary interventions	9 (18.4 %)	5 (11.4 %)	0.346
Follow-up (months)	25 (14, 28)	36 (23, 44)	<0.001
LwRA/EDG distance	HR (n=49)	Non-HR (n=44)	Total (n=93)
≤ 2 mm	40 (81.6%)	26 (59.1%)	66 (71.0%)
2-4 mm	7 (14.3%)	14 (31.8%)	21 (22.6%)
≥5mm	2 (4.1%)	4 (9.1%)	6 (6.5%)

HOR: Hybrid operating room, non-HOR: mobile 2D fluoroscopic imaging system

Continuous data are presented as the median (Inter Quartile Range) and categorical data as counts (percentage)

* distance between the LwRA (Lowest renal artery) and endograft (EDG) measured on postoperative CTA after aortic curvilinear reconstruction

Table 4 Details of secondary interventions of 93 patients undergoing EVAR stratified by the type of imaging system used during procedure

	Indication	Time from procedure
HOR group (n=49)		
Iliofemoral bypass (n=1)	Acute lower limb ischemia	6 days
Groin hematoma drainage (n=1)	Groin hematoma	16 days
Iliac limb thrombectomy (n=1)	Iliac limb occlusion	2 months
Palmaz stenting (n=1)	Type IA endoleak	4 months
Adjunctive iliac limb (n=1)	Type IB endoleak	7 months
Transcaval embolization (n=2)	Type II endoleak	8 and 24 months
Surgical endograft explantation (n=1)	Endograft occlusion	13 months
Fenestrated cuff (n=1)	Thoraco-abdominal aneurysm	19 months
Non-HOR group (n=44)		
Translombar embolization (n=1)	Type II endoleak	13 months
Iliac limb thrombectomy (n=1)	Iliac limb occlusion	19 months
Common femoral endarterectomy (n=1)	Chronic limb ischemia	25 months
Crossover femorofemoral bypass (n=1)	Iliac limb occlusion	39 months
Fenestrated cuff (n=1)	Type IA endoleak	43 months

HOR: Hybrid operating room, non-HOR: mobile 2D fluoroscopic imaging system